УДК 550.34: 621.039.9

LOCATION AND IDENTIFICATION OF SEISMIC EVENTS AROUND NORTH KOREAN NUCLEAR TEST SITE FOLLOWING THE 3 SEPTEMBER 2017 UNDERGROUND NUCLEAR TEST

W.-Y. Kim, D. Schaff, P.G. Richards

Lamont-Doherty Earth Observatory, Columbia University, New York, U.S.A.

At least thirteen small seismic events that occurred close to and following the North Korean underground nuclear test (UNT) on 3 September 2017 were detected and located by using seismic waveform data from regional stations. Other than the first event, widely reported to be a cavity collapse, the magnitudes of these shocks range from 2.3 to 3.6. Based on their timing, and proximity to the UNTs, these shocks may be considered as aftershocks. They are located within 1 km of each other with small relative location errors, approximately 50 m. We assess a method to classify each of these small events separately based on their spectral amplitude ratios derived from regional P- and S-waves. We examine additional possible small seismic events around the North Korean test site by using seismic data from stations in South Korea, Russia, and northeastern China including IMS seismic arrays, GSN stations, and national network stations. A linear discriminant function based on Mahalanobis methods applied to P/S spectral ratios does a better job of screening events than does a simple average of such ratios.

INTRODUCTION

Following the large underground nuclear test (UNT) of 3 September 2017 in North Korea, a number of smaller seismic events were detected by use of a template and cross-correlation (see below). The first such event, which occurred about 8.5 minutes after the UNT, is now recognized as a collapse event (e.g., [1]). Additional small seismic events, at or close to the North Korean test site, followed this same UNT. On September 23, 2017, 20 days after the UNT, a magnitude 3.6 event occurred, and a dozen small shocks followed in the region. In this study we apply a P/S spectral ratio method of event identification to explore the capability of such methods at the lowest magnitudes for which they are likely to have utility.

Most of our waveform data for event detection and identification was acquired by broadband three-component stations; the open station MDJ in northeastern China (operated as part of a collaboration between the China Earthquake Administration and the U.S. Geological Survey), the station USA0B in Russia (operated as part of the International Monitoring System's seismic array at Ussuriysk), and the borehole station YNCB (Yeoncheon) in South Korea situated close to the demilitarized zone (DMZ) between the two Koreas, and a dozen additional stations in South Korea operated by KMA (Korea Meteorological Administration) (Figure 1). We have found and analyzed in some detail the 13 aftershocks listed in Table.

Table. Seismic events that occurred around North Korean test site since September 3, 2017[(a)]

Event id	pair	Date (year-mo-dy)	Time (hr:mm:ss)	Latitude (°N)	Long. (°E)	h (km)	Mag (M_L)	CC 0923	Ref[(b)]
1		2017-09-03	03:38:31.5	41.343	129.036	1.5	4.2	0.27	USGS
2	A	2017-09-23	04:43:00.0	41.350	129.060	4.0	2.7	0.57	KMA
3	A	2017-09-23	08:29:16.8	41.296	129.044	2.5	3.6	1.00	USGS
4	A	2017-10-12	16:41:08.3	41.375	129.050	3.3	3.2	0.67	LDEO
5	A	2017-12-01	22:45:56.0	41.31	129.11	5.0	2.4	0.50	KMA
6	B	2017-12-05	14:40:53.0	41.32	129.13	5.0	2.9	0.48	KMA
7	B	2017-12-05	19:55:55.9	41.32	129.13	5.0	2.3	0.32	LDEO
8	C	2017-12-09	06:13:35.0	41.32	129.10	5.0	3.3	0.26	KMA
9	C	2017-12-09	06:40:02.0	41.31	129.11	5.0	2.8	0.18	KMA
10	C	2018-02-06	10:53:53.0	41.33	129.10	5.0	2.8	0.37	KMA
11	D	2018-02-07	21:46:01.0	41.32	129.09	5.0	3.2	0.35	KMA
12	D	2018-02-07	21:46:23.9	41.32	129.09	5.0	3.3	0.30	LDEO
13	D	2018-02-08	17:39:17.8	41.32	129.09	5.0	2.4	0.32	LDEO

[(a)] h = depth fixed in location; Mag=local magnitude; CC=detection cross-correlation coefficient; 0923=template event 2017/09/23, 08:29;
[(b)] Event locations are taken from reports by USGS=National Earthquake Information Center, US Geological Survey, KMA=Korea Meteorological Administration, and LDEO=this study

1. Detection of small seismic events around North Korean test site

The waveform cross-correlation (CC) detector is known to lower the seismic event detection threshold by about one magnitude unit or more, below what is normally detected through standard processing (e.g., [2–4], among others). We used 3-component records at two stations, MDJ (Δ=369 km, Az=6º) and USA0B (Δ=398 km, Az=36º), from the shock on 2017-09-23 at 08:29 (event #3, Table) as a template event, to detect additional small events. The template 3-component waveforms were taken as 80 s long for MDJ and 85 s long for USA0B. Template traces start about 1 s before the P arrival through 30 s and 32 s after Lg arrivals for MDJ and USA0B, respectively. The records are filtered between 0.8 and 8 Hz to avoid undesired noise. Large signal durations (T) and wide frequency bandwidths (B) are the key for a robust correlation detector [5] suggested that a time-bandwidth product (T ×B) exceeding 100 (or smaller TB with more stations) is necessary for reliable event attribution. We use three-component records and take the mean of the cross-correlation scores from the three components to enhance the robustness of event detection. The local magnitude (M_L) of the events we identified with the CC detector, on or near the North Korea test site, were determined from the RMS (root mean squared) amplitudes of detected signals in the time windows and calibrated to the amplitudes of the template traces with known magnitude.

To determine CC threshold values above which to claim a detection, we used the method described by [6] which enables making detections having a predetermined false alarm rate. In this method the continuous waveform data are searched twice, using a time-reversed template as well as the time-forward template. These have the same time-bandwidth product, and generate similar distributions of noise-driven low CC values. We found that CC values above 0.15 for MDJ, and above 0.2 for USA0B, arose only from the forward template, and were thus plausible candidate detections of waveforms similar to the template. We set these values as our detection thresholds for each 3-component template.

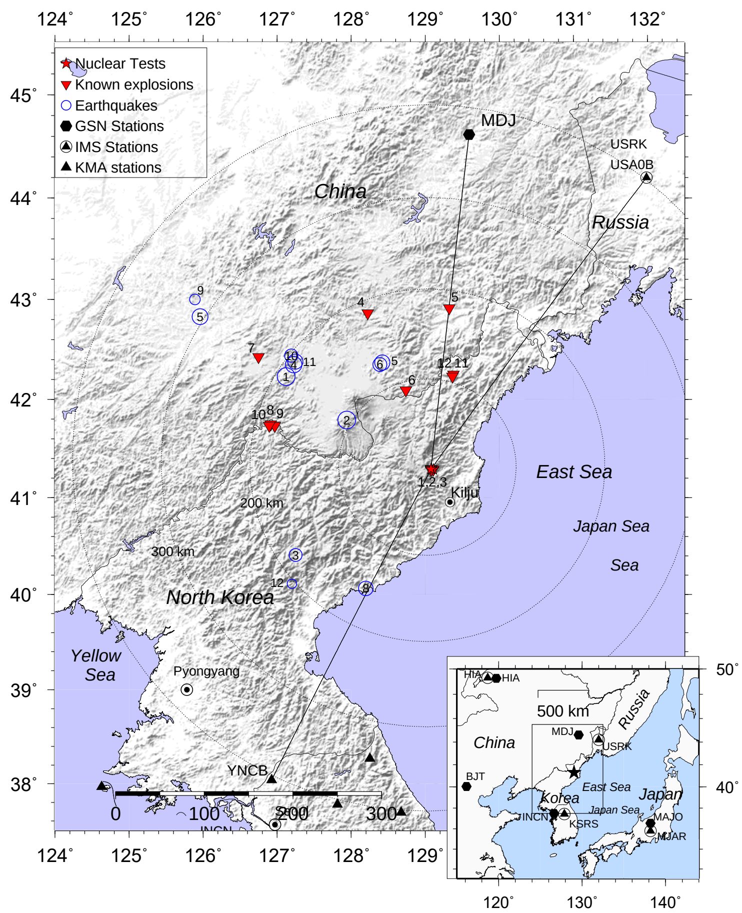

Figure 1. A map showing the location of North Korean nuclear tests (stars), earthquakes (open circles), single-hole explosions and large industrial explosions (inverted triangles), and seismographic stations (triangles) in the northeastern Korean peninsula and in northeast China. Dotted circles concentric with the North Korean test site have radii 100, 200, and 300 km

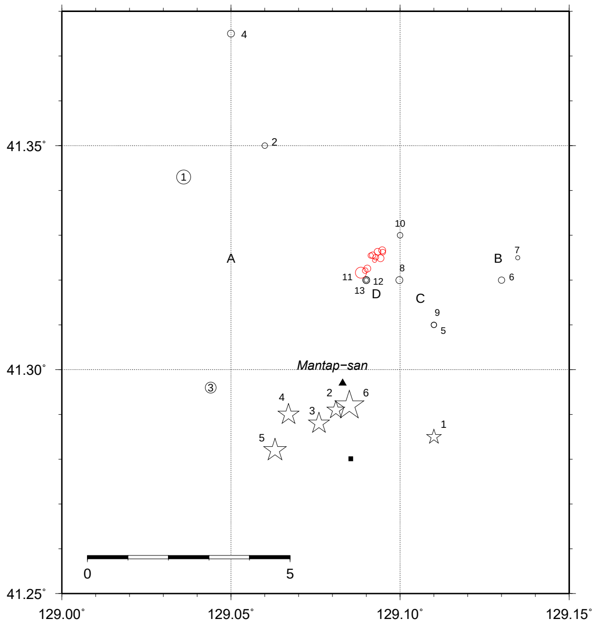

Figure 2. A map showing the location of North Korean nuclear tests (open stars) and preliminary locations of aftershocks (circles) with event id & doublet pairs as given in Table. Event pairs are indicated by A through D. Relocated aftershocks are plotted by red circles, whose sizes are proportional to event magnitudes. 11 accurately relocated aftershocks (event #2 through #12 in Table) shows that they are in fact located all much closer together

We detected 26 events by using the 2017-09-23 (08:29) MDJ 3-component templates with a threshold of 0.15 from 2017 September 3 to 2018 March 1, whereas the USA0B 3-component templates detected 32 events that exceed the threshold of 0.2 from 2017 September 3 to 2017 December 31. Note that USA0B data is available for analysis from IDC (International Data Center, CTBTO) archive via vDEC (Virtual Data Exploitation Centre) with about three months delay. We select events by associating detection time at two stations such that MDJ and USA0B detection times are within 4.0±1.0 s. We found 11 common detections from the two stations. Their magnitude ranged between 2.3 and 4.2 (magnitude of the template event is M_L 3.6).

Examination of waveform quality of the detected events indicated that 10 of them could be located by traditional methods. Specifically we used P and S arrival times at regional stations in the distance range 350-600 km together with the HYPOINVERSE location code [7]. Due to a lack of station coverage, several events are located with their initial location set at KMA or USGS reported ones, and we fixed the depth at 5 km. We thus obtained what we regard as preliminary absolute locations for 13 aftershocks, as indicated in Table and plotted in Figure 2. Their location error ellipses at 95% confidence level are very large. 11 accurately relocated aftershocks (event #2 through #12 in Table) by using late arrival Lg wave at regional stations shows that they are in fact located all much closer together – within about 1 km (Figure 2).

2. CHARACTERIZATION OF SMALL EVENTS AROUND NORTH KOREAN TEST SITE

There are a number of new stations available to characterize seismic events in and around the northern Korean peninsula and northeastern China, as well as the open stations MDJ, INCN; and IMS stations USRK and KSRS. But most of these stations lack a waveform archive going back far enough to allow us to assemble training data for the discrimination analysis. Hence, MDJ is still the station of choice with its archive of data starting in the late-1980s. The broadband 3-component station USA0B, which is the reference site of the IMS array USRK (Ussuriysk, Russia), has acquired data since the fall of 2008. Vertical-component records from these shocks recorded at USA0B (Δ ~370 km) are shown in Figure 3.

To identify each of these events (earthquake, or explosion) we followed Kim et al. [8], which assembled training data from 12 earthquakes and 12 explosions that occurred within about 200 km from North Korea's UNTs. In that paper, *P/S* spectral amplitude ratios were used as a basic discriminant and linear discriminant functions (LDFs) combined these ratios taken at different frequencies. It was found that the combination from four discrete frequencies, at 6, 7, 8, and 9 Hz, provided the best discrimination between explosions and earthquakes, using *P/S* ratios. However, in this study we use frequencies 6 to 10 Hz, since these 13 aftershocks are larger than the event studied in [8], and have signals with good signal-to-noise ratios at higher frequencies.

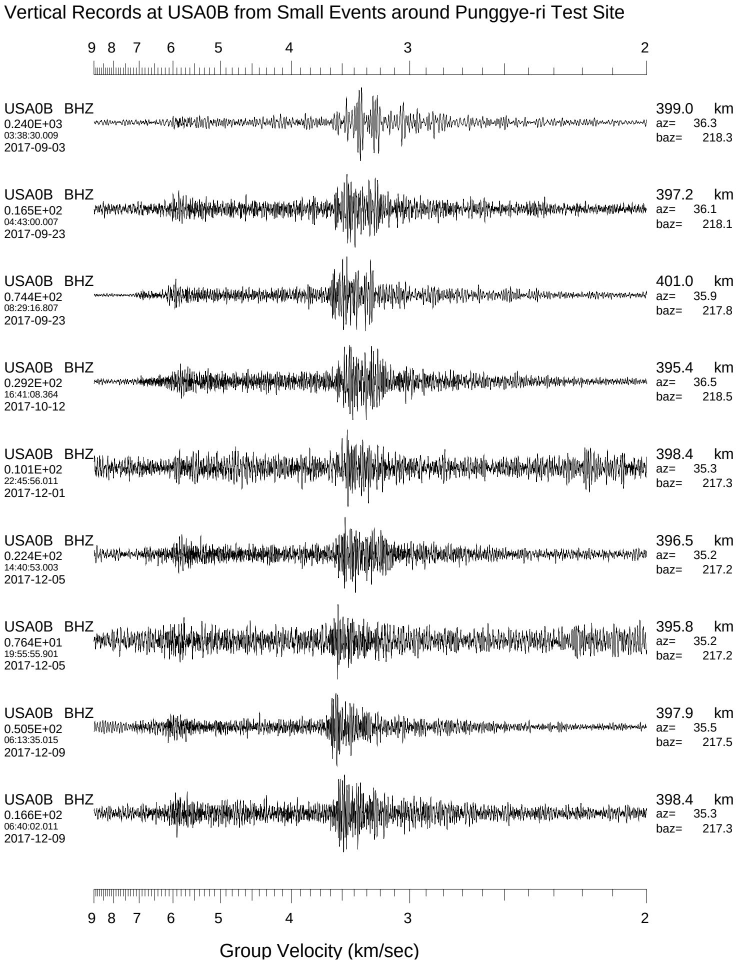

Figure 3. Vertical component seismic records bandpass filtered 1−15 Hz from the first nine seismic events recorded at USA0B station. Records show Pg– and Lg–wave arrivals consistent with the events located close to each other. Pg–waves centered at group velocity 5.8 km/s (~69 s) and Lg-waves centered at group velocity 3.3 km/s (~121 s) are used to measure P/S spectral ratios

To identify each of these events (earthquake, or explosion) we followed Kim et al. [8], which assembled training data from 12 earthquakes and 12 explosions that occurred within about 200 km from North Korea's UNTs. In that paper, *P/S* spectral amplitude ratios were used as a basic discriminant and linear discriminant functions (LDFs) combined these ratios taken at different frequencies. It was found that the combination from four discrete frequencies, at 6, 7, 8, and 9 Hz, provided the best discrimination between explosions and earthquakes, using *P/S* ratios. However, in this study we use frequencies 6 to 10 Hz, since these 13 aftershocks are larger than the event studied in [8], and have signals with good signal-to-noise ratios at higher frequencies.

2.1. *P/S* spectral amplitude ratio on three-component records

Previous efforts to distinguish explosions from earthquakes on the basis of seismographic data have demonstrated that the high-frequency *P*/*S* spectral ratios of rotated, three-component regional records have greater discrimination power than vertical-component records alone (e.g., [9]. Hence, we apply that previous experience to data analysis for small seismic events which occurred around the North Korea test site since Sept. 2017. We rotate the observed NS- and EW-component seismogram pairs to obtain radial (R) and tangential (T) components. The *P*/*S* ratios of three-component records are then formed for each station by defining $P\ /\ S = (P_Z^2 + P_R^2)^{1/2}\ /\ (S_Z^2 + S_R^2 + S_T^2)^{1/2}$ where subscripts indicate the component as described by [8]. For example, P_Z indicates the spectral amplitude of *P* waves on the vertical-component (Z), and S_R indicates the spectral amplitude of *S*-waves on the radial-component. A single three-component *P*/*S* ratio is obtained for each discrete frequency. Our approach builds on the observation that explosive sources tend to excite relatively strong and impulsive *P* waves and weak shear waves, whereas earthquakes as shear-dislocation sources tend to generate weak *P* waves but relatively energetic *S* waves, particularly on the transverse component. By using all three components the discriminant is improved because it does a better job of evaluating the *S*-wave, than use of the vertical component alone.

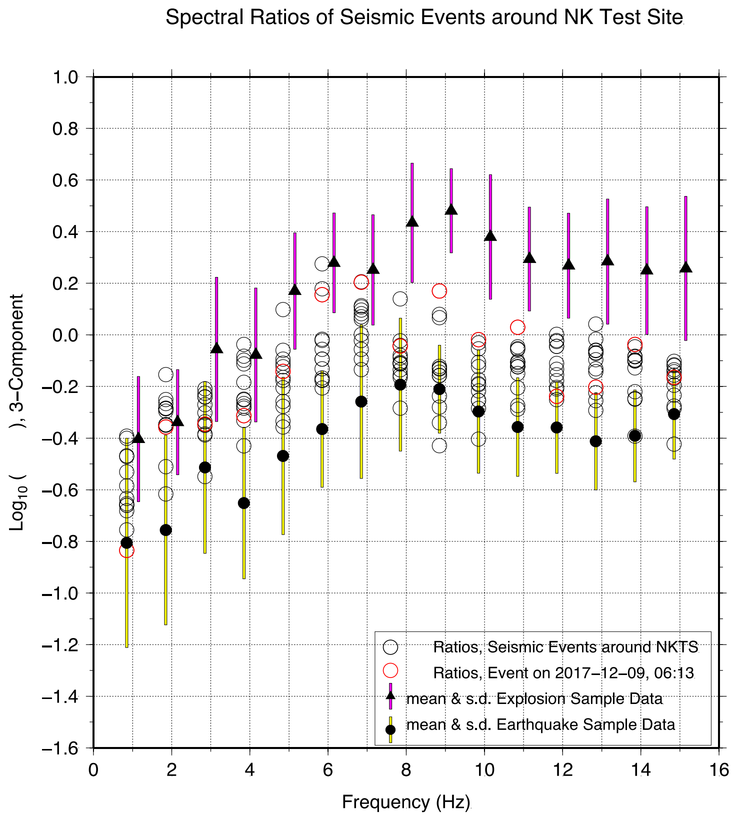

Figure 4. Three-component log_{10}(Pg/Lg) spectral amplitude ratios at discrete frequencies between 1 and 15 Hz used in classification are plotted for 13 events (circles). The data used for the analysis are all from MDJ. A mean spectral value for each discrete frequency point of the training events is plotted both for earthquakes (black circle) and for explosions (black triangle), with a bar representing the scatter (±1 S.D.). Note that most of the measured spectral ratios fall into the earthquake population, but ratios from some events lie in the explosion population. P/S ratios from event #8 are plotted in red to illustrate details of its observed P/S ratios

Figure 4 shows three-component $\log_{10}(Pg/Lg)$ spectral amplitude ratios at discrete frequency points between 1 and 15 Hz used to characterize the 13 small events that occurred around the North.

Korean test site. The vertical bars in Figure 4 are the standard deviations of earthquake and explosion populations of the sample data, representing the range of spectral ratios for the training events. We attempt to classify the 13 aftershocks by using *P/S* ratios obtained first from the three-component recordings and using the LDF obtained by using five discrete frequencies 6, 7, 8, 9 and 10 Hz with the same training event data as in Kim et al. (2017). For each event, let three-component $\log_{10}(Pg/Lg)$ ratios at frequencies of 6, 7, 8, 9 and 10 Hz correspond to the variables r_1, r_2, r_3, r_4, and r_5. The linear discriminant function we obtain, is.

$$D(\mathbf{r}) = -4.73 + 19.05r_1 - 16.58r_2 - 13.27r_3 + 55.51r_4 - 9.99r_5 \quad (1)$$

For this LDF, the Mahalanobis distance measure is $\Delta^2 = 27.1$ and the misclassification probability is 0.47%. By applying the equation to the three-component *P/S* ratios from 13 small events, we found that two events – #8 (2017/12/09, 06:13) and #12 (2018/02/07, 21:46:23) (Table), are classified as explosions whereas 11 events are classified as earthquakes as shown in Figure 5.

Thus, in 3-component LDF analyses, 11 events can be classified as earthquakes based on their *P/S* ratios, and their discriminant scores are clustered within the earthquake population (Figures 4). But events 8 and 12 appear problematic, since their discriminant scores are even to the right of the classification line (where the discriminant score is close to zero). Event #8 is classified as an explosion via the higher-quality analysis associated with three-component data (Figure 5), even though its waveforms are very comparable to those of event #9.

Obviously, the two events with discriminant scores close to the classification line appear to have relatively strong *P* radiation compared to *S*-waves, in contrast to the analysis for 11 other aftershocks. The *P/S* spectral ratios shown in Figure 4 have peaks between 6–9 Hz for event #8, which is the main frequency band we used for discrimination analysis using LDF. Hence, those ratio peaks will classify this event as an explosion. However, at frequencies higher than 10 Hz, the spectral ratios of event #8 fall into the earthquake population.

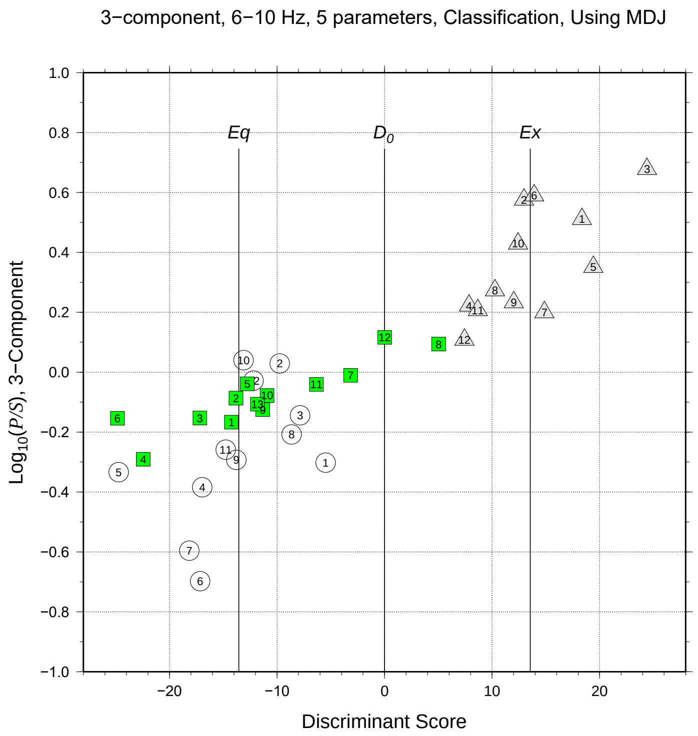

Figure 5. Classification analysis of the 3-component P/S ratio from 13 seismic events are carried out by using five frequencies: 6, 7, 8, 9, and 10 Hz and using the linear discriminant function obtained for MDJ with the same training data as in [8], 11 events (green squares) are classified as earthquakes; and two events are classified as explosions (8 & 12). Discriminant scores of 13 events are plotted with their mean $log_{10}(Pg/Lg)$ ratios. All the training data − 12 earthquakes (circles) and 12 explosions (shaded triangles) plotted as reference, provide discrimination power with the Mahalanobis distance of Δ^2 = 27.1, and the total misclassification probability of 0.47%. Vertical lines denoted as Eq and Ex are the projection of the multivariate means of the earthquake and explosion population, respectively. The vertical line D_0 is the classification line. Event ids are as listed in Table

The seismic records at MDJ from events #8 and #9 (which were only about 26 minutes apart) are very similar, having a CC value of 0.66 for waveforms in the passband from 0.8 to 8 Hz. So these events must originate within a quarter wavelength of each other (~0.33 km) and they were separated by only about 26 minutes in time. However, their *P/S* ratios are remarkably different, as the discrimination score of event #9 is close to the centroid of earthquake population (the *Eq* line in Figure 5), whereas #8 is classified as an explosion.

The seismic records from event #12 are somewhat contaminated by signals from event #11 that occurred only about 23 s previously (Table), and hence, their *P/S* ratios and discrimination score fall close to the classification line (D_0, see Figure 5). Note that the two populations are also quite well separated by mean 3-component $\log_{10}(Pg/Lg)$ ratio equal to about –0.1 (events #8 and #12 being exceptions) (see Figure 5).

2.2. Network averaged P/S spectral amplitude ratio on three-component records

We analyzed additional seismic records at stations with distances and path properties similar to those of MDJ − namely, USA0B (Δ=398 km, Az=36º) and YNCB (Δ=410 km, Az=207º), see Figure 1 − to see if this changed the identification results obtained from MDJ data. The network-averaged three-component $\log_{10}(Pg/Lg)$ spectral amplitude ratios for the 13 seismic events from stations MDJ, USA0B and YNCB are plotted with circles in Figure 6. In Figure 6, a mean spectral value for each discrete frequency point of the training events used to form the LDF is plotted, both for earthquakes (*black circle*) and for explosions (*black triangle*), with a colored bar representing the scatter (±1 S.D.) as reference. This use of network averaged three-component data achieves better separation of the explosion and earthquake populations than was found in Figure 4, which was based on three-component data at MDJ station only.

Network-averaged 3-component *P/S* ratios calculated with these additional two stations were used to classify events 1 through 9, now using three stations, and events 10 through 13, using two stations – MDJ and YNCB. All events are classified as earthquakes as shown in Figure 7. As demonstrated in [9], high-frequency regional *P/S* ratios provide much better discrimination power when a network of stations is available.

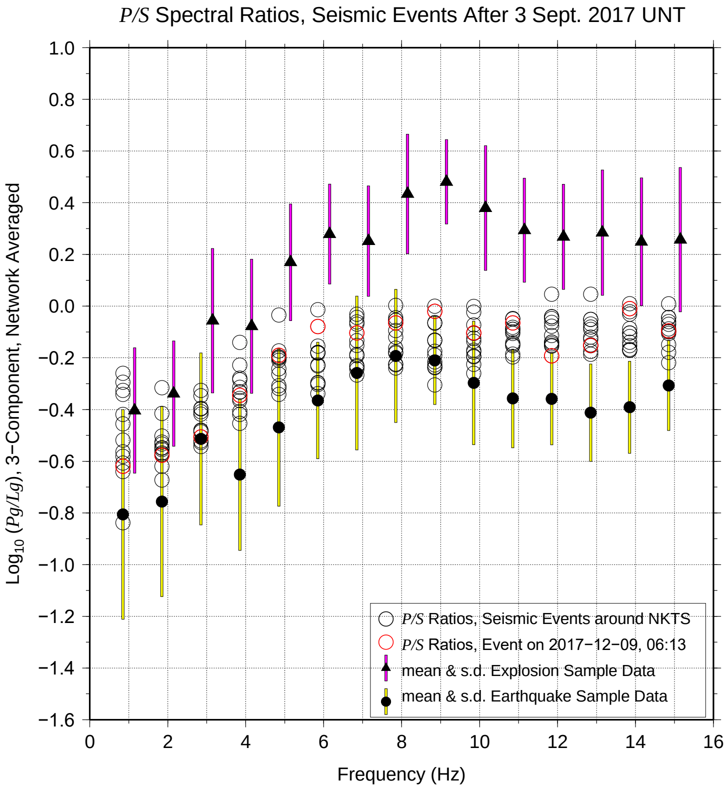

Figure 6. Similar to Figure 4 but now using network averaged three-component $log_{10}(Pg/Lg)$ spectral amplitude ratios. The spectral ratio data for the 13 seismic events at MDJ are plotted with circles. A mean spectral value for each discrete frequency point of the training events used to form the LDF is plotted, both for earthquakes (black circle) and for explosions (black triangle), with a colored bar representing the scatter (±1 S.D.). This use of network averaged three-component data achieves better separation of the explosion and earthquake populations than was found in Figure 4, which was based on three-component data at MDJ station only

3. Discussion and Conclusions

Following the North Korea UNT of 2017 September 3 in North Korea, a series of seismic events were reported by KMA and USGS, and other agencies, and taken up by the news media. The first of these seismic events occurred about 8.5 minutes after the UNT, and is now recognized as a cavity collapse with seismic magnitude about 4. A pair of nearby events occurred on 2017 September 23 (at 08:29 with magnitude 3.6, at first misidentified as explosive by a unit in China though later reports declared that it was probably an earthquake; and KMA also reported an earlier and smaller shock on the same day, event #2 at 04:43 – see Table).

We applied a waveform cross-correlation detector to continuous data from two three-component broadband stations (open station MDJ and the International Monitoring System station USA0B), using signals from event #3 as templates. Among the 13 events that we detected and analyzed, there are four doublets – 2 & 3 (A), 6 & 7 (B), 8 & 9 (C), and 11 & 12 (D)(see Table). Each pair exhibits very similar waveforms having cross-correlation values well above the detection threshold of 0.15 we have used with MDJ data to declare detections. For example, the doublet A (2 & 3) has CC values of 0.67, whereas doublet B (6 & 7) has CC values 0.48 and 0.32. Hence, the overall sequence of aftershocks included some distinct doublets, rather than all occurring as a single large multiplet. The first seven events have similar waveforms based on their high CC values, then the last six events have lower CC values than the first group. Hence, the two large events - #3 (M 3.6, 2017-09-23, 08:29) and #8 (M 3.3, 2017-12-09, 06:13) are the two end members of the sequence. In the first two months of the sequence, events occurred at an interval of about 20 days; then the interval between events detected in Dec. 2017 (events #5 through #9) became short, only 4–5 days; and finally for events in Feb. 2018 the inter-event time was very short (~ 1 day).

The analysis presented in this paper has obtained good results, in that we have been able to identify all of the aftershocks we have detected as being earthquakes, on the basis of their *P/S* spectral ratios. Note that our whole approach (with a high-performance event detector) has enabled working with events so small (at magnitudes around 3 they would be on the order of a tenth of a kiloton in yield if they were explosions, which we strongly doubt), that their signal quality is quite low. A network of stations was required for a robust application of classical Mahalanobis methods.

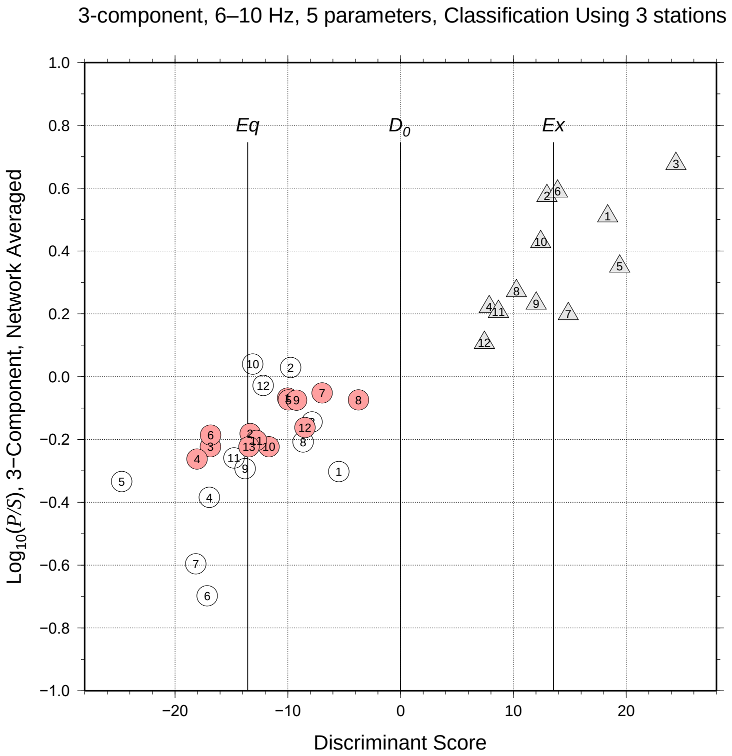

Figure 7. Similar to Figure 5, but now the classification is done with network averaged, three-component log10(Pg/Lg) spectral ratios at five discrete frequencies between 6 and 10 Hz. Using the linear discriminant function obtained for MDJ in [8], all 13 seismic events are classified as earthquakes (red filled circles). The discriminant scores of 12 earthquakes (circles) and 12 explosions (shaded triangles) of the training data are plotted with their mean log10(Pg/Lg) ratios for reference

An overall conclusion is that damage from shock waves of the large UNT of 2017 September 3 has led to slow adjustments in the surrounding region, entailing stress relief (via aftershocks), occurring on a distributed string of rock fractures.

Acknowledgments. We thank the staff at IDC, CTBTO in Vienna, Austria – Randy Bell and Ivan Kitov in particular, who kindly assisted us to acquire waveform data from the IDC archive by using the vDEC. Our work has been supported by the Consortium for Verification Technology under Department of Energy/ National Nuclear Security Administration award DE-NA0002534 via a subcontract between Columbia University and the University of Michigan, and by the Defense Threat Reduction Agency under award HDTRA-1-11-1-00027. This is Lamont-Doherty Earth Observatory contribution number xxxx**.**

REFERENCES

1. Tian, D. Collapse and earthquake swarm after North Korea's 3 September 2017 nuclear test, in press / D. Tian, J. Yao, L. Wen // Geophysical Research Letters, 2018.
2. Gibbons, S. J. The detection of low magnitude seismic events using array-based waveform correlation Geophys / S. J. Gibbons, F. Ringdal // J. Int., 2006. – 165, no. 1. – P. 149 – 166, doi: 10.1111/j.1365-246X.2006.02865.x.
3. Kim, Won-Young Induced seismicity associated with fluid injection into a deep well in Youngstown, Ohio / Won-Young Kim // J. Geophys. Res., 2013. – V. 118, Is. 7. - P. 3506 - 3518, doi:10.1002/jgrb.50247.
4. Schaff, D.P. Semiempirical statistics of correlation-detector performance / D.P. Schaff // Bull. Seism. Soc. Am., 2008. – 98. – P. 1495–1507.
5. Harris, D. B. A waveform correlation method for identifying quarry explosions / D. B. Harris // Bull. Seism. Soc. Am., 1991. – 81. – P. 2395–2418.
6. Slinkard, M. D. Multistation validation of waveform correlation techniques as applied to broad regional monitoring / M. Slinkard, D.Schaff, N. Mikhailova, S. Heck, C. Young, P. G. Richards // Bull. Seism. Soc. Am., 2014. – 104. – P. 2768–2781.
7. Klein, F. W. User's guide to HYPOINVERSE-2000, a Fortran program to solve for earthquake locations and magnitudes / F.W. Klein, U.S. // Geol. Surv. Open File Rep., 2007.- 02-171. – 121 pp.
8. Kim, Won-Young Evaluation of a seismic event, 12 May 2010, in North Korea / Won-Young Kim, Paul Richards, David Schaff, Karl Koch // Bull. Seism. Soc. Am., 2017.– 107, No. 1, February 2017, doi: 10.1785/0120160111.
9. Kim, W. Y. Discrimination of earthquakes and explosions in southern Russia using regional high-frequency three-component data from the IRIS/JSP Caucasus Network / W. Y. Kim, V. Aharonian, A. L. Lerner-Lam, P. G. Richards // Bull. Seism. Soc. Am., 1997. – 87. – P. 569–588.

2017 ЖЫЛҒЫ 03 ҚЫРКҮЙЕКТЕГІ ЖЕРАСТЫ ЯДРОЛЫҚ ЖАРЫЛЫСТАН КЕЙІН СОЛТҮСТІК КОРЕЯНЫҢ ЯДРОЛЫҚ СЫНАУЛАР ПООЛИГОНЫ ЖАНЫНДАҒЫ СЕЙСМИКАЛЫҚ ОҚИҒАЛАРДЫ ЖЕРГІЛІКТЕУ ЖӘНЕ СӘЙКЕСТЕНДІРУ

Ким В.-Й., Шафф Д.Р., Ричардс П. Г.

Колумбия университетінің Ламонт-Доэрт жер обсерваториясы, Нью-Йорк, АҚШ

Солтүстік Кореяда жерасты ядролық жарылыстар жерлері жанында 2016 ж. 9 қыркүйекте және 2017 ж. 03 қыркүйекте болған кемінде он төрт кіші сейсмикалық оқиғалар, аймақтық станцияларда сейсмикалық сигналдардың толқындық түрлері туралы деректердің көмегімен, айқындалып жергіліктелген. Осы оқиғалардың магнитудасы 2,3–3,5 аралығында. Осы оқиғалар жерасты ядролық жарылыстар (ЖЯЖ) полигоны жанында болғанына сүйене, оларды афтершоктр ретінде санауға болады. Осы оқиғалардың эпиорталықтары, жергіліктеудің 50 м. қателігімен, бір бірінен 1 км. қашықтығында орналасқан. Авторлар осы кіші оқиғаларды дискримнациялау үшін ең жақсы әдісі ретінде – P және S аймақтық толқындардың спектрлік амплитудаларының қатынасын қоладанған. P/S спектрлік амплитудаларының қатынасы бойынша осы оқиғалардың біреуіде жарылысқа ұқсайтын болып сәйкестендірілмейді.
Қосымша ретінде, ЯСЖТШҰ Халықаралық мониторингі жүйесінің (IMS) сейсмикалық топтарын, жаһандық сейсмографиялық желінің GSN станцияларын, сондай-ақ аймақтық желінің станцияларын қоса алғанда, Онтүстік Корея мен солтүстік-шығыс Қытайдағы сейсмикалық станциялардың деректерін пайдаланып, Солтүстік Кореяның сынау полигоны төңірегіндегі ықтимал әлсіз сейсмикалық оқиғалары зерделенген. P/S спектрлік қатынастарға қолданылған, Махаланобис әдісінде негізделген сызықтық дискриминанттық функция, сондай қатынастардың арифметикалық орта мәнінен, оқиғаларды қадағалау үшін жақсырақ жарайтыны туралы қорытынды жасалған.

ЛОКАЛИЗАЦИЯ И ИДЕНТИФИКАЦИЯ СЕЙСМИЧЕСКИХ СОБЫТИЙ ВБЛИЗИ ПОЛИГОНА ЯДЕРНЫХ ИСПЫТАНИЙ СЕВЕРНОЙ КОРЕИ ПОСЛЕ ПОДЗЕМНОГО ЯДЕРНОГО ИСПЫТАНИЯ 3 СЕНТЯБРЯ 2017 ГОДА

Ким В-Й., Шафф Д.Р., Ричардс П.Г.

Ламонт-Дохертская обсерватория Земли Колумбийского университета, Нью-Йорк, США

Как минимум тринадцать малых сейсмических событий, произошедших вблизи места подземных ядерных испытаний в Северной Корее 3 сентября 2017 г., было обнаружено и локализовано с использованием волновых форм сейсмических сигналов на региональных станциях. Кроме первого события, о котором сообщалось как об обрушении полости, магнитуда малых сейсмических событий варьируется от 2,3 до 3,6. Основываясь на времени и близости этих событий к подземному ядерному испытанию (ПЯВ), их можно рассматривать как афтершоки. Эпицентры данных событий расположены в 1 км друг от друга с погрешностью локализации примерно в 50 м. Авторы оценили возможности метода классификации каждого из этих малых событий на основе спектральных отношений амплитуд региональных волн P и S.
Дополнительно изучены возможные слабые сейсмические события в окрестности испытательного полигона Северной Кореи с использованием данных сейсмических станций в Южной Корее, России и северо-восточном Китае, включая сейсмические группы Международной системы мониторинга ОДВЗЯИ (МСМ), станций глобальной сейсмографической сети GSN, а также станций региональной сети. Сделан вывод о том, что линейная дискриминантная функция, основанная на методе Махаланобиса, примененная к спектральным соотношениям P/S, лучше подходит для отслеживания событий, чем среднее арифметическое значение таких соотношений.